Citation: Rowane, A. J., Mallepally, R. R., Gavaises, M. & McHugh, M. A. (2020). Interfacial tension of isomers n-hexadecane and 2,2,4,4,6,8,8-heptamethylnonane at high pressures and temperatures. Industrial & Engineering Chemistry Research, 59(19), pp. 9293-9299. doi: 10.1021/acs.iecr.0c00213

This is the accepted version of the paper.

This version of the publication may differ from the final published version.

Subscriber access provided by Virgina Commonwealth University Libraries & VIVA (Virtual Library of Virginia)

Thermodynamics, Transport, and Fluid Mechanics

Interfacial tension of isomers n-hexadecane and 2,2,4,4,6,8,8-heptamethylnonane at high pressures and temperatures

Aaron James Rowane, Rajendar R. Mallepally, Manolis Gavaises, and Mark A. McHugh

Ind. Eng. Chem. Res., **Just Accepted Manuscript** • DOI: 10.1021/acs.iecr.0c00213 • Publication Date (Web): 17 Apr 2020

Downloaded from pubs.acs.org on April 17, 2020

Just Accepted

“Just Accepted” manuscripts have been peer-reviewed and accepted for publication. They are posted online prior to technical editing, formatting for publication and author proofing. The American Chemical Society provides “Just Accepted” as a service to the research community to expedite the dissemination of scientific material as soon as possible after acceptance. “Just Accepted” manuscripts appear in full in PDF format accompanied by an HTML abstract. “Just Accepted” manuscripts have been fully peer reviewed, but should not be considered the official version of record. They are citable by the Digital Object Identifier (DOI®). “Just Accepted” is an optional service offered to authors. Therefore, the “Just Accepted” Web site may not include all articles that will be published in the journal. After a manuscript is technically edited and formatted, it will be removed from the “Just Accepted” Web site and published as an ASAP article. Note that technical editing may introduce minor changes to the manuscript text and/or graphics which could affect content, and all legal disclaimers and ethical guidelines that apply to the journal pertain. ACS cannot be held responsible for errors or consequences arising from the use of information contained in these “Just Accepted” manuscripts.

is published by the American Chemical Society. 1155 Sixteenth Street N.W., Washington, DC 20036

Published by American Chemical Society. Copyright © American Chemical Society. However, no copyright claim is made to original U.S. Government works, or works produced by employees of any Commonwealth realm Crown government in the course of their duties.

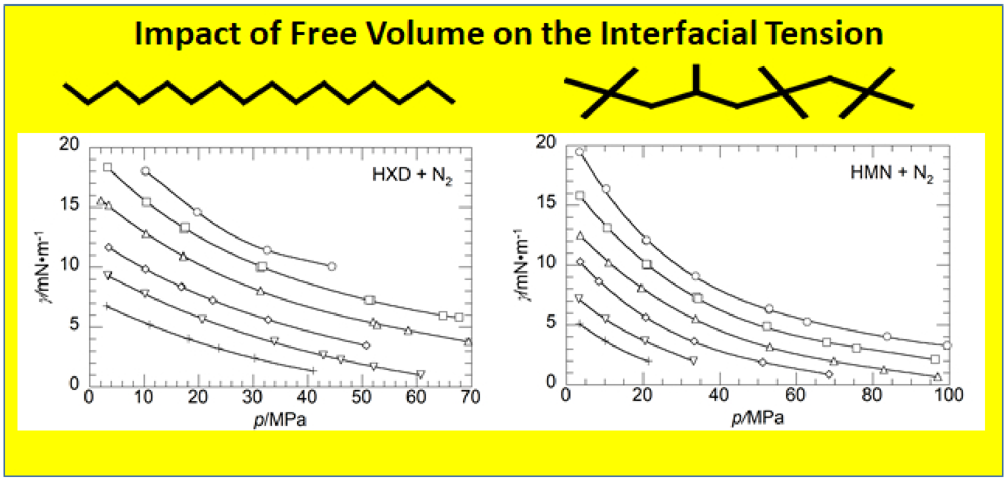

113x54mm (144 x 144 DPI)

Interfacial tension of isomers *n*-hexadecane and 2,2,4,4,6,8,8-heptamethylnonane at high pressures and temperatures

Aaron J. Rowane[a,*] , Rajendar R. Mallepally[b], Manolis Gavaises[a], Mark A. M^c^Hugh[b]

[a] Department of Mechanical Engineering and Aeronautics, City University of London,
Northampton Square, ECIV 0HB London, UK

[b] Department of Chemical and Life Science Engineering, Virginia Commonwealth University,
601 W Main St, Richmond, VA, 23284, USA

* Corresponding author; e-mail: aaronrowane@gmail.com

Abstract

Highly branched alkanes exhibit enhanced free volume relative to their straight chain analogs leading to increased solubility of sparingly soluble gases, such as N_2, as well as lower hydrocarbon-gas interfacial tension (IFT) values. In this study high-pressure, high-temperature (HPHT) IFT data are reported for two C16 isomers, hexadecane (HXD) and heptamethylnonane (HMN), with N_2 from ~298 to 573 K and pressures to 100 MPa. The IFT data are modeled with Density Gradient Theory (DGT) in conjunction with the Perturbed-Chain, Statistical Associating Fluid Theory equation of state (EoS) with pure component parameters calculated with three different group contribution (GC) methods. One GC method (B-GC) is developed from a database of high-pressure density data and the other two GC methods (S-GC and T-GC) are developed from a large database of pure component vapor pressure and saturated liquid density data. DGT calculations incorporating the B-GC method reasonably represent the IFT for both HXD + N_2 and HMN + N_2 at low temperatures, but result in significant deviations from experimental IFT values

at high temperatures. The S-GC method provides improved IFT predictions relative to the B-GC method at high temperatures, but S-GC predictions are inferior to those obtained using the T-GC method. The superior performance of the T-GC method is attributed to the use of second order GC parameters and to the ability of this method to more correctly predict EoS parameters for both normal and branched alkanes.

Key words: PC-SAFT, Density Gradient Theory, Diesel Surrogates, *n*-hexadecane, 2,2,4,4,6,8,8-heptamethylnonane

1. Introduction

n-hexadecane (HXD) and 2,2,4,4,6,8,8-heptametylnoane (HMN) are often identified as diesel fuel surrogates[1] since they are from two prominent classes of compounds found in diesel fuel. HXD and HMN are also used as reference fuels to determine the cetane number of diesel fuel using ASTM D613[2]. An important issue for the efficient operation of a diesel engine is the droplet formation obtained from the breakup of the fuel spray injected into the combustion chamber. For example, Hiroyasu et al.[3] show that when the fuel is initially injected into the diesel combustion chamber and exposed to air, the Sauter Mean Diameter (SMD) of the fuel droplets depends directly on the viscosity, density, and interfacial tension (IFT) of the fuel. The present study focusses on the measurement of IFT data for two C16 isomers, HXD and HMN, with N_2 at temperatures from 298 to 573 K and pressures up to 100 MPa. To avoid potential combustion reactions during an IFT experiment, inert N_2 is used as a representative surrogate for air given that N_2 and O_2 are both diatomic gases exhibiting similar intermolecular potentials.

Interestingly, it has been conjectured that the fuel + air mixture in the combustion chamber transitions into a supercritical fluid mixture characterized by the disappearance of the gas-liquid interface, enhanced gas-liquid mass transfer, and zero latent heat of vaporization[4]. Supercritical diesel injection could potentially reduce emissions, minimize pollutant formation, and ultimately increase engine efficiency[5]. This transition is strongly dependent on the fuel droplet size since mass and heat transfer processes have to occur rapidly enough, relative to the pre-combustion lifetime of the fuel, for the fuel-air mixture to cross into the critical region. The IFT data from the present study obtained with surrogate fuel-air mixtures provide considerable insight on the fate and properties of the diesel spray as a consequence of operating parameters. In addition, the data reported here can be used to verify and refine the computational fluid dynamics tools used to map changes in the composition, temperature, and pressure of the fuel within the injector nozzle and combustion chamber.

Currently there are only a handful of IFT studies available for binary *n*-alkane + N_2 mixtures[6-11] at high-pressure, high-temperature (HPHT) conditions. In fact, to the best of our knowledge, there are no studies reporting IFT data for binary *i*-paraffin + N_2 mixtures. It is important to note that the pressure-temperature space reported in the available *n*-alkane + N_2 IFT studies is severely limited due to the challenges associated with HPHT measurements. To address these challenges several IFT techniques have been adapted to operate at HPHT conditions including the pendant drop[6-8, 11], capillary rise[9, 12], capillary wave[10], and maximum bubble pressure[13] methods. Although saturated liquid and vapor mixture density data are needed to accurately interpret IFT data, in many instances these data are not available and, thus, it becomes problematic standardizing and evaluating IFT literature data. For example, Garrido et al.[8] utilized the pendant drop technique to measure IFT data for mixtures of ethanol, 2-methoxybutane, and hexane each with N_2, for temperatures up to 333 K and pressures up to 15 MPa. These authors assumed the liquid and vapor phase mixture densities are equal to the densities of pure heavy component and pure N_2. Alternatively, Reno and Katz[9] employed the capillary rise technique to measure IFT data for *n*-butane + N_2 and *n*-heptane + N_2 mixtures for temperatures up to 358 K and pressure up to 7 MPa. These authors estimated values for the saturated liquid and vapor densities using a technique described in detail elsewhere.[14] Niño Amézquita et al.[11] utilized the pendant drop method to measure IFT data for *n*-heptane + N_2 mixtures for temperatures up to 373 K and pressures up to 10 MPa. These authors obtained saturated liquid and vapor densities from NIST data tables. Dechoz and Rozé[10] employed a capillary wave technique to measure IFT data for heptane + (N_2, Ar, or CO_2) and diesel fuel + N_2 mixtures for temperatures up to 348 K and pressures up to 10 MPa. These authors derived vapor and liquid densities using refractive index information. Currently, only the studies by Zolghadr et al.[7], Jianhua et al.[6], and Pereira et al.[12] reported IFT data using experimental saturated liquid and vapor mixture densities. Both Zolghadr et al. and Jianhua et al. utilized the pendant drop technique for IFT measurements. Zolghadr et al. reported IFT data for (*n*-heptane, *n*-hexadecane, or diesel) + N_2 mixtures for temperatures up to 393 K and pressures up to 40 MPa. Jianhua et al. reported IFT data for mixtures of *n*-alkanes ranging from five to eight carbons + N_2 and toluene + N_2 for temperatures at 313 K and pressures up to 40 MPa. Pereira et al. utilized the capillary rise technique for *n*-decane + (N_2, CH_4, or CO_2) mixtures. In the present study the pendant drop method is used to measure IFT data for C16 isomers, HXD and HMN, with N_2 at temperatures from 298 to 573 K and pressures up to 100 MPa. Here the resultant IFT data are interpreted using previously reported saturated liquid mixture densities[15] and with saturated vapor densities estimated using the PC-SAFT EoS. The HXD + N_2 IFT data are directly compared to the data reported by Zolghader et al. as a means of verification of the HPHT technique used in the present study. The impact of pressure on the IFT data in the present study is compared to the trends reported by Zolghadr et al. and to the trends reported by

Pereira et al. for *n*-decane + N_2 since this system is expected to behave in a similar manner to the of HXD + N_2 system.

IFT data measured in this study are modeled using Density Gradient Theory (DGT), proposed by Cahn Hillard[16], accompanied by an equation of state (EoS). Pereira et al.[12] employed DGT in conjunction with the Peng-Robinson EoS to predict the IFT of binary mixtures of *n*-decane + (N_2, CH_4, or CO_2). Niño Amézquita et al.[11] and Liu et al.[17] each utilized DGT in conjunction with the Perturbed-Chain Statistical Associating Fluid Theory (PC-SAFT) EoS to model IFT data of light hydrocarbon + N_2 mixtures. In the present study DGT is used with the PC-SAFT EoS to model both HXD + N_2 and HMN + N_2 IFT data. Pure component PC-SAFT parameters are calculated using the group contribution (GC) method of and Burgess and coworkers[18] (B-GC), Sauer and coworkers[19] (S-GC), and Tihic and coworkers[20] (T-GC). Both Tihic and coworkers and Sauer and coworkers[19] derived GC parameters by regressing pure component, saturated vapor pressure and liquid densities while Burgess derived GC parameters by regressing only high-pressure density data. A significant difference between the S-GC and T-GC methods is that Tihic and coworkers incorporated second order group contribution parameters for branched alkanes while Sauer and coworkers did not. The modeling results presented here provide a measure of the sensitivity of the DGT calculations on the use of different GC methods using the PC-SAFT EoS.

2. Materials and Methods

2.1. Materials

Table 1 lists the source and mass fraction purity of all the chemicals investigated in this study which are used as received.

Table 1. Chemicals used in this study listed with the source and mass fraction purity reported by the manufacturer.

Chemical Name	Source	Mass Fraction Purity	Analysis method[a]
n-Hexadecane	Sigma-Aldrich	0.990	GC
2,2,4,4,6,8,8-Heptamethylnonane	Acros Organics	0.980	GC
Nitrogen	Air-Gas	1.000	

[a] Determined by gas chromatography (GC) by the supplier.

2.2. High-Pressure, High-Temperature Pendant Drop Tensiometer

Figure 1 is a schematic diagram of the HPHT Pendant Drop Tensiometer (HPHT-PDT) used in this study. The aerial view of the apparatus shows a gas delivery cell, a liquid delivery cell, and a viewing cell where IFT measurements are carried out. Details on the variable-volume liquid and gas delivery cells are found in previously reported phase behavior studies[15]. The viewing cell, constructed from Inconel 718, has a 1.588 ± 0.005 cm internal diameter and a length of 1.270 ± 0.005 cm, which equates to an internal volume of approximately 10 cm^3. This cell is fitted with opposing sapphire windows (Hemlite sapphire, 1.905 cm thick x 1.905 cm outside diameter ± 0.005 cm, faces flat to ± 0.0008 cm and parallel to ± 0.0025 cm, and beveled edges 0.762 cm x 45°, GT Crystal Systems, LLC) that allow for the contents to be monitored using a camera and light source adapted from the KRÜSS Drop Shape Analyzer 25E (DSA25E). Although not shown here, the entire apparatus is situated on a table with pneumatic vibration isolators for active vibration dampening that eliminates the impact of external vibrations on the IFT measurements. All of the cells are typically disassembled and cleaned off-line before each experiment. In addition, since IFT results can be skewed by the presence of slight impurities, the transfer lines and valves, are cleaned thoroughly by flushing with hexane, then acetone, and then heated to evaporate any residual solvent. Upon reassembly, the entire setup is flushed with N_2 three times to remove any air and moisture that may remain in the system. The liquid delivery cell is then loaded with the solute of interest and the valve connecting the liquid delivery cell to the viewing cell is closed. Next the gas delivery and viewing cells are loaded with N_2 simultaneously by opening the valve between these cells during the loading process.

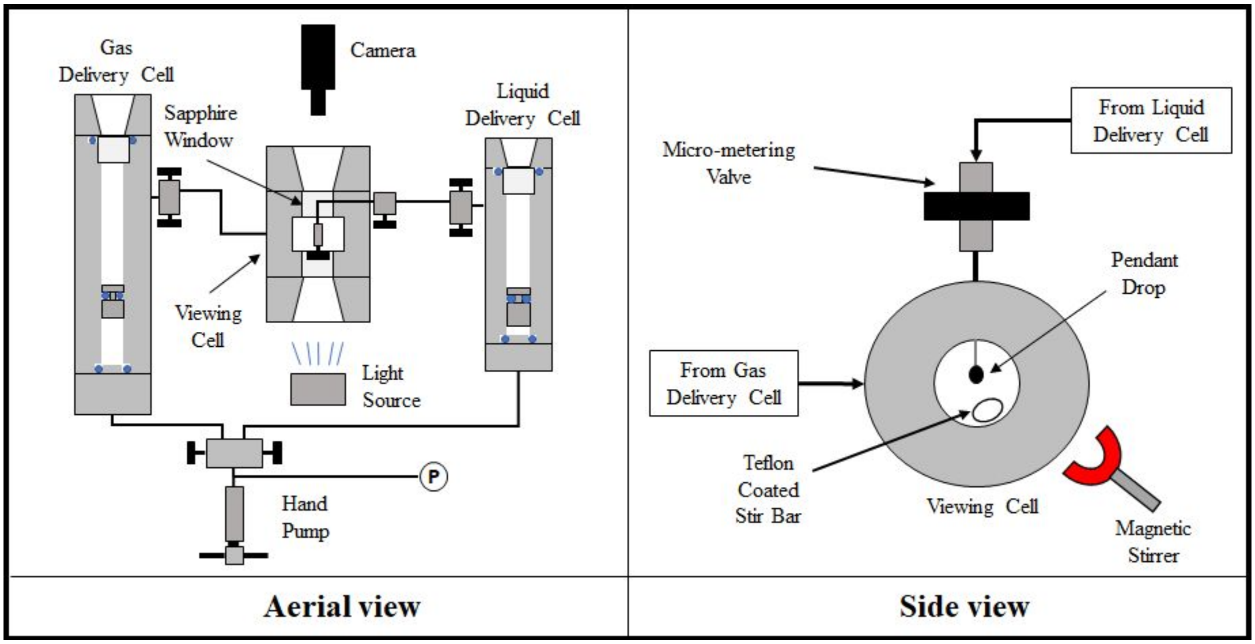

Figure 1. Schematic diagram of the high-pressure, high temperature pendant drop tensiometer used in this study.

The internal volumes and, hence, pressure of the fluids of interest in both the gas and liquid delivery cells are adjusted using a high-pressure hand pump (model 37-5.75-60, HIP Inc.) that delivers or removes water to the back end of each cell. The two-way valve at the outlet of the hand pump allows for pressurization or depressurization of the gas delivery and liquid delivery cells either independently or simultaneously. The pressure is measured with two transducers (model 245-BFS, accurate to ±0.03 MPa to 35 MPa and model 245-BZS, accurate to ±0.34 MPa, for pressures to 345 MPa, Viatran Corp.) located in the water line directly before the two-way valve at the outlet of the hand pump. The valve between the gas delivery and viewing cell always remains open to enable monitoring and adjusting the viewing cell pressure. Conversely, the valve between the liquid delivery and viewing cell remains closed until IFT measurements are performed. The liquid delivery cell is maintained at a maximum temperature of 373 K when operating at high pressures to prevent solidification of HXD. The gas delivery cell is not heated and remains at room temperature throughout an experiment. The micro-metering valve is heat traced and maintained at the same temperature as the fluid in the viewing cell. The internal temperatures of the liquid delivery and viewing cell are measured using type-K thermocouples calibrated against a standard (BetaProbe 238 TI+, precision to 0.01 K, accuracy to 0.06 K, Martel Electronics 239 Corp.). Both the liquid delivery and viewing cells are heat traced and insulated. However, for any given isotherm, the temperature of the viewing cell can drift due to the long measurement times associated with the pendant drop technique. The maximum deviation of the viewing cell temperature is within 0.4 K for a complete isothermal set of IFT measurement.

Prior to a series of IFT measurements, approximately 1 to 2 cm^3 of HXD or HMN are charged to the viewing cell, which is then adjusted to the desired pressure and temperature while mixing vigorously for approximately 20 minutes to equilibrate the liquid and vapor phases in the cell. As explained by Berry et al.[21] the accuracy of the pendant drop technique hinges on attaining the largest possible drop volume. Here a pendant drop is dosed from the blunt end of a 1.562 mm diameter high-pressure needle that communicates with the micro-metering valve located just before the viewing cell. The micro-metering valve allows for carefully displacing the residual liquid in the valve to maximize the droplet volume.

In this study the droplet profile is evaluated using the KRÜSS ADVANCE software package that employs an asymmetric drop shape analysis (ADSA) routine. Equation 1 is used to determine the interfacial tension between the liquid and vapor phases, γ,

$$\gamma = \frac{\Delta\rho g R_0^2}{\beta} \tag{1}$$

where $\Delta\rho$ is the density difference between the saturated liquid and vapor phases, g is the acceleration due to gravity, R_0 is the maximum horizontal diameter of the pendant drop, and β is the dimensionless shape factor determined numerically from the droplet profile. Both R_0 and β are values evaluated by the Kruss ADVANCE software[22]. The value for R_0 depends on a scaling factor determined by knowing the needle diameter measured to ±0.001 mm with a micrometer. The accuracy of the parameter β is dependent on how closely the numerical procedure can match the droplet profile. However, $\Delta\rho$ is an input that needs to be determined independently. In this study the liquid phase density, ρ_{liq}, is obtained from experimental (HXD or HMN) + N_2 density data previously reported by our group[15]. The nitrogen rich, saturated vapor phase densities, ρ_{vap}, are estimated using the PC-SAFT EoS[23] with parameters calculated using exclusively the GC method of Tihic et al.[20], and with binary interaction parameters fit to our previously measured experimental HPHT vapor-liquid phase behavior data[15]. Additional statistical information is provided in the SI showing that the T-GC method provides superior density predictions for both N_2 + HXD and N_2 + HMN systems when the best fit k_{ij} parameter is used.

The Kruss ADVANCE software allows for real-time monitoring of the IFT and the droplet volume. Once the pendant drop is formed, both the IFT and droplet volume are monitored for up to 10 minutes to ensure sufficient time for the droplet to equilibrate with the surrounding saturated gas phase. For each measurement the IFT is sampled every six seconds, for ten minutes, to ensure that the value for the IFT does not fluctuate significantly. In the present study 94 out of 102 reported IFT data points are stable within ±0.03 mN/m over the course of the 10 min measurements sequence.

3. Experimental results

The IFT data are obtained at pressures chosen in random order for a given isotherm to minimize any potential experimental artifacts in the measurements. Figures 2(a) and 2(b) show the impact of pressure and temperature on the interfacial tension of HXD + N_2 and HMN + N_2 mixtures, respectively. Note that the IFT values for the HMN + N_2 system are singinificantly lower than those for the HXD + N_2 system especially at higher pressures. The lower IFT values for the HMN + N_2 system are a direct result of the increased solubility of N_2 in the saturated liquid phase which was measured in a previous investigation[15]. These larger IFT values for the HMN system further supports our previous claim that HMN exhibits a larger free volume in comparison to HXD at the same temperature-pressure conditions[15]. A more in depth discussion comparing HMN and HXD free volumes and data tables listing experimental IFT values at each temperature and pressure are included in the supporting information.

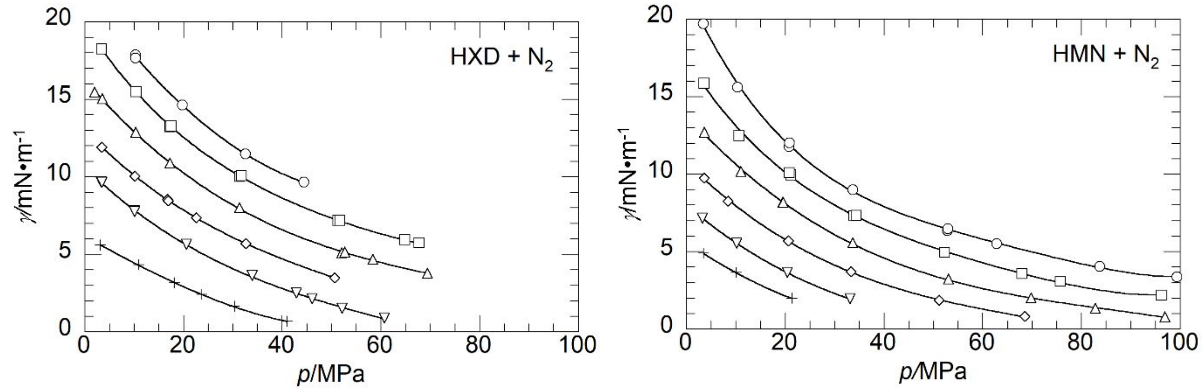

(a) (b)

Figure 2. Effect of pressure and temperature on the interfacial tension of N_2 + (a) *n*-hexadecane at ○ - 324.0, □ - 375.1, △ - 426.3, ◇ - 478.8, ▽ - 530.0, and × - 571.9 K and (b) 2,2,4,4,6,8,8-heptamethylnonane at ○- 325.9, □ - 377.6, △ - 430.0, ◇ - 480.1, ▽ - 530.2, and × - 570.7 K.

3.1 Comparisons to Literature Data

Figure 3 is a deviation graph comparing IFT data for the HXD + N_2 system obtained in this study to those obtained by interpolating the dataset of Zolghadr et al.[7] Figure 3 shows that in all cases the IFT values reported in the present study are 2 to 8% greater than the interpolated values from the dataset of Zolghadr et al. Currently, no other IFT data exist for the HXD + N_2 system for comparison. It is worthwhile to compare the trends in the IFT with increasing pressure for data obtained in the present study and data from Zolghadr and coworker's study, and from Pereira and coworkers' study. Figure 2 shows that the isothermal *γ-p* curves for both the HXD +N_2 and HMN + N_2 systems smoothly decrease exponentially with increasing pressure. Figures 4(a) and 4(b) show the same isothermal *γ-p* curves for data obtained by Zolghadr et al. for the HXD + N_2 system and data obtained by Pereira et al.[12] for the *n*-decane + N_2 system. Zolghadr and coworkers' HXD

+ N_2 curves initially decay linearly with pressure up to approximately 10 MPa where they exhibit a kink and change slope although the curves once again decay linearly up to 40 MPa. In contrast, Pereira and coworkers's *n*-decane + N_2 curves smoothly decrease exponentially with increasing pressure, which more closely follows the trends observed in the present study for both the HXD + N_2 and HMN + N_2 systems. The trends in the γ-p data of the present study also mirror those reported by Jianhua et al.[6] for (*n*-pentane, *n*-hexane, *n*-octane, and *n*-decane) + N_2 and by Garrido et al.[8] for *n*-hexane + N_2. It is worth noting that Zolghadr and coworkers also report IFT data for heptane + N_2 that also show a kink and change in slope in the γ-p curves. The IFT data reported in the present study and the data reported by Pereira and coworkers are obtained after the liquid and vapor phases in the viewing cell are mixed to achieve equilibrium. In contrast Zolghadr and co-workers do not include a mixing, pre-equilibration step in their IFT measurement procedure. The lack of mixing and pre-equilibration is likely the reason for the observed differences in the trends observed by Zolghadr and co-workers compared to those observed in the present study and by Pereira and coworkers.

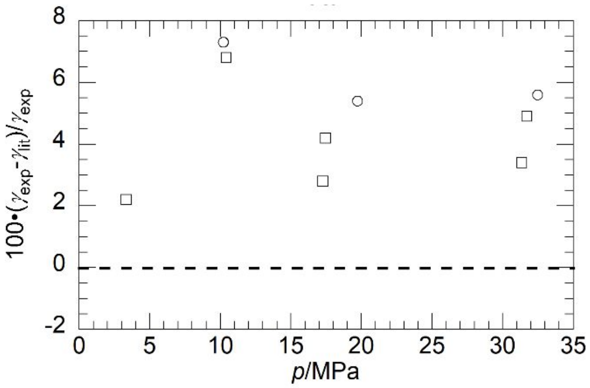

Figure 3. Comparison of IFT data for the HXD + N_2 system obtained in this study, γ_{exp}, to data of Zolghadr et al.[7], γ_{lit}, at ○- 324.0 K and □ - 375.1 K. Data by Zolghadr and coworkers are interpolated results.

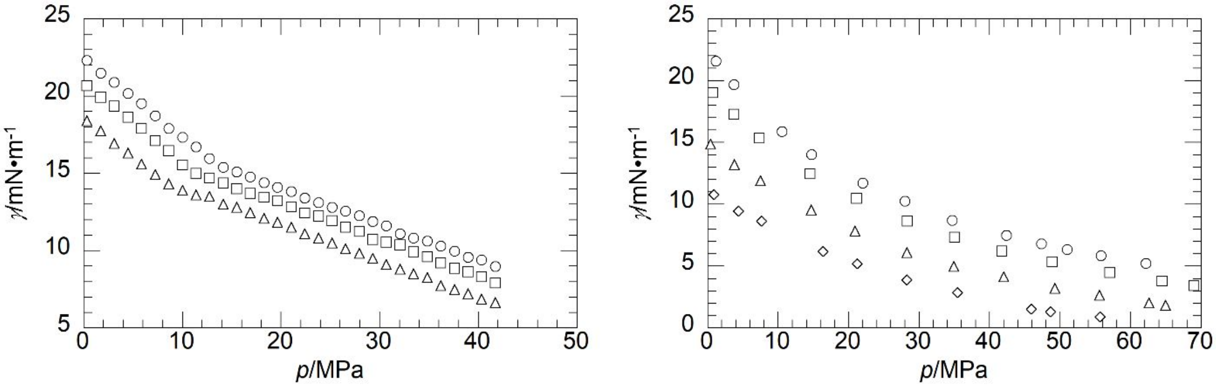

(a) (b)

Figure 4. Impact of pressure and temperature on the interfacial tension. (a) HXD + N_2 data reported by Zolghadr et al.[7] at ○ - 313.15 , □ - 353.15, and △ - 393.15 K and (b) decane + N_2 data reported by Pereira et al.[12] at ○ - 313.4 , □ - 343.2, △ - 392.6, and 442.2 K.

3.2 Modeling IFT data using Density Gradient Theory coupled with the PC-SAFT EoS

Density Gradient Theory (DGT) proposed by Cahn and Hilliard[16] is an IFT predictive model that has been used extensively in the literature for hydrocarbon + N_2 systems. However, to the best of our knowledge DGT has not been used to model IFT data for branched paraffin + N_2 mixtures due to the absence of experimental data for these systems. DGT takes into account the local composition gradient at the interface of a two-phase system where the Helmholtz free energy is non-homogenous. Predictions with DGT require a *pVT* EoS; here the PC-SAFT EoS is used similar to the approach used by Liu et al.[17] and Mairhofer and Gross.[24] Details on DGT and the

PC-SAFT EoS are only highlighted here and the reader is directed elsewhere[17, 23, 24] for more detailed descriptions of these two models.

The PC-SAFT EoS requires values for *m*, the segment length, *σ* the segment diameter, and *ε*/*k* the segment energy for each component in the mixture. These parameters are calculated using three GC methods to assess the impact of these different methods on the calculated IFT values using DGT. One GC method, described by Burgess et al.[18] (B-GC), regressed group parameters by fitting pure component, high pressure density data. In contrast the other two GC methods, described by Sauer et al.[19] (S-GC) and by Tihic et al.[20] (T-GC), regressed group parameters by fitting a large database of pure component vapor pressures and saturated liquid densities. Table 2 lists PC-SAFT parameters calculated using each GC method and those reported by Gross and Sadowski[21], which are obtained by fitting pure component vapor pressure and saturated liquid density data. Note that HXD parameters calculated using the T-GC method are in close agreement with those reported by Gross and Sadowski in contrast with those calculated using the B-GC and S-GC methods. It is not surprising that the B-GC EoS parameters differ significantly from the Gross and Sadowski parameters since Burgess and coworkers regressed compressed liquid density data rather than vapor pressure and saturated liquid density data to develop their method. It is worth noting that the S-GC ϵ/k value for HMN is closer to those for cyclic or aromatic compounds rather than those for branched and normal alkanes as reported by Gross and Sadowski. The superior performance of the T-GC method relative to the S-GC method is likely due to the second order GC parameters Tihic uses for branched alkanes and that Tihic independently fit normal and branched alkane data while Sauer combined both data sets to generate GC parameters. Although HMN PC-SAFT parameters are not available in the literature for direct comparison to GC calculated parameters, the large discrepancies between HXD S-GC and Gross and Sadowski parameters suggest that fitting combined normal and branched alkane data potentially skews the resultant GC parameters for both chemical families.

Table 2. Calculated PC-SAFT EoS parameters *m*, σ, and ε/k for HXD and HMN using and Burgess'[18], Sauer's, and Tihic's[20] GC methods and parameters for HXD and N_2 taken directly from Gross and Sadowski[23].

	B-GC Parameters			S-GC Parameters			T-GC Parameters		
Component	*m*	σ/Å	(ε/k)/K	*m*	σ/Å	(ε/k)/K	*m*	σ/Å	(ε/k)/K
HXD	10.220	3.4218	241.8	7.609	3.8637	237.54	6.669	3.944	253.59
HMN	9.743	3.5767	256.4	5.009	4.2774	284.79	5.603	4.164	266.46
Gross and Sadowski									
HXD	6.649	3.9552	254.70						
N_2	1.205	3.3130	90.96						

The performance of the DGT is expected to be sensitive to the ability of the PC-SAFT EoS to accurately predict HXD + N_2 and HMN + N_2 phase behavior (pressure-composition isotherms) and the resultant saturated liquid and gas densities. Since nonzero values for k_{ij} are typically needed for an accurate description of the phase behavior, the DGT calculations presented here incorporate non-zero k_{ij} values obtained from the best fit of pressure-composition isotherms using the S-GC and T-GC methods reported previously by our group[15]. The SI shows phase behavior calculations using the B-GC[18] method, which was not reported previously. DGT requires values for the influence parameter, c_{ii}, for each component in the mixture. Here c_{ii} is used as a temperature-independent parameter consistent with the approach found in other literature studies[11, 17, 24]. Each component c_{ii} value is expected to depend on the GC method used with the PC-SAFT EoS and, therefore, c_{ii} values are obtained by fitting the DGT to the IFT data reported in this study. The influence parameter for N_2 is the literature value obtained from a fit of N_2 surface tension data using the DGT with the PC-SAFT EoS[17]. Table 3 lists the binary interaction parameters and influence parameters used in this study. Additionally, table 3 lists the c_{ij} value for HXD reported by Marihofer and Gross obtained from a fit of pure HXD surface tension data. It is interesting to note that the best fit c_{ij} value using the T-GC method is reasonably close to that reported by Mairhofer and Gross[24]. The DGT calculations presented in this study are performed using commercially available software, VLXE[25].

Table 3. Binary interaction parameters, k_{ij}, from a fit of high-pressure, high-temperature binary phase behavior data for the HXD + N_2 and HMN + N_2 systems[15] and influence parameters, c_{ii}, from the best fit of IFT data for the HXD + N_2 and HMN + N_2 systems.

HXD

	k_{ij}	c_{ii}•10^{19}/J•m^5•mol^{-2}
B-GC	-0.0125	13.800
S-GC	0.1250	30.000
T-GC	0.1190	22.500
Mairhofer and Gross[24]	-	24.183

HMN

B-GC	-0.0328	12.000
S-GC	0.1250	13.500
T-GC	0.1300	15.000

N_2

Liu et al.[17]	-	0.054

Figure 5 shows DGT + PC-SAFT IFT predictions and performance details for the N_2 + HXD and N_2 + HMN systems. The left-hand side panels in figure 5 show predicted IFT curves for each GC method compared to experimental data and panels on the right-hand side show the temperature variation of the average, absolute deviation, Δ_{AAD} (equation 2), for each GC method. Here the B-GC method provides reasonable predictions at lower temperatures, but significantly overpredicts IFT values as the temperature increases. The S-GC method provides slightly greater Δ_{AAD} values at lower temperatures compared to the B-GC method, but the S-GC performs significantly better at higher temperatures. Of the three GC methods, the T-GC method provides the best overall performance for both the HXD + N_2 and HMN + N_2 systems with reasonable Δ_{AAD} values at each temperature and significantly lower Δ_{AAD} values than both the B-GC and S-GC methods at the highest temperatures investigated in this study. Burgess et al. report that their GC method offers increased accuracy for high pressure compressed liquid density predictions at the expense of poor vapor pressure predictions. Hence, the reasonable performance of the B-GC method at low temperatures and poor performance at high temperatures may be due to an inaccurate description of vapor densities saturated with HXD or HMN. Although not shown here it is interesting that vapor densities predicted with all three GC methods do not vary more than 2% at temperatures up to 430 K. However, at temperatures above 430 K, vapor densities predicted using the S-GC and T-GC methods are up to 30% greater than those predicted using the B-GC method, which means the B-GC method underpredicts the concentration of HXD or HMN in the vapor phase leading to a larger liquid-vapor density difference and a larger IFT. In general, the better performance of the T-GC method relative to the S-GC method is likely due to Tihic's more accurate representation of EoS parameters for branched alkanes through the use of second order group parameters. As noted earlier the T-GC method also better represents HXD EoS parameters relative to the S-GC method which ultimately leads to improved IFT results over the entire temperature range considered in this study.

$$\Delta_{AAD}/\% = 100 \cdot \frac{1}{N}\sum_{i=1}^{N}\left|\left(\frac{x_{i,exp}-x_{i,cal}}{x_{i,exp}}\right)\right| \qquad (2)$$

where $x_{\mathrm{i,exp}}$ represents an experimental IFT data point, $x_{\mathrm{i,calc}}$ represents a calculated IFT data point, and *N* is the number of data points.

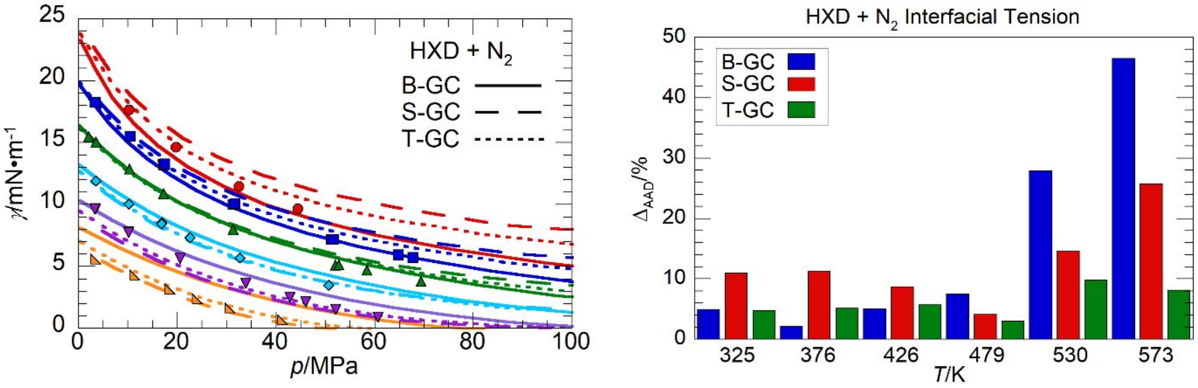

(a)

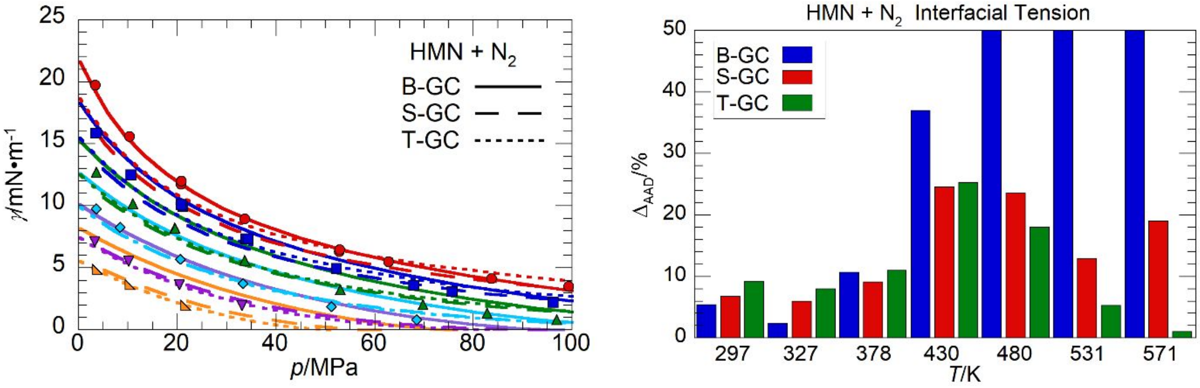

(b)

Figure 5. Comparison of experimental IFT data for (a) N_2 + HXD at ● - 324.6, ■ - 375.5, ▲ - 426.1, ◆ - 478.6, ▼ - 530.4, and ◣ - 572.7 K and for (b) N_2 + HMN at ● - 326.5, ■ - 377.9, ▲ - 429.8, ◆ - 479.8, ▼ - 530.5, and ◣ - 571.4 K. Panels on the left-hand side compare DGT + PC-SAFT predictions (lines) to experimental data points. Panels on the right-hand side show the variation of the absolute average deviation (Δ_{AAD}) with temperature.

4.Conclusions

Interfacial tension data for HXD + N_2 and HMN + N_2 mixtures are reported from 298 to 573 K and up to 100 MPa. HXD and HMN are two industrially relevant fluids as they often serve as surrogates for diesel fuel and as reference fuels. The differences in the reported data for the C16 isomers demonstrates how paraffin chain branching significantly reduces the IFT in the presence of a sparingly soluble gas. The lower IFT values for the HMN + N_2 system are a direct consequence of the increased N_2 solubility in liquid HMN relative to HXD reported in our previous study[15]. DGT in conjunction with the PC-SAFT EoS provides a reasonable representation of the HPHT IFT data obtained in this study when the EoS parameters are calculated with the T-GC method. The DGT + PC-SAFT model using parameters calculated using the B-GC method provides reasonable performance at low temperatures where the concentration of HXD or HMN in the vapor phase remains low, but the performance quickly deteriorates as the temperature and HXD or HMN concentration increases in the vapor phase. The better performance of the T-GC method relative to the S-GC method can be attributed to the incorporation of second order groups used in the T-GC method to calculate EoS parameters for branched alkanes.

Supporting Information

The supporting information includes a justification as to why the T-GC method was chosen to estimate vapor phase densities to interpret the IFT data, data tables listing IFT data for both HXD and HMN, PC-SAFT phase equilibria calculations using the B-GC method, and an in-depth discussion on the free volume differences between HXD and HMN.

Acknowledgments

The authors thank Joseph Roos, Joseph Remias, Joshua Moore, Ashu Gupta, and Mark Devlin, all at Afton Chemical Corporation, for their helpful technical insight with this study.

References

1. Mueller, C. J.; Cannella, W. J.; Bays, J. T.; Bruno, T. J.; DeFabio, K.; Dettman, H. D.; Gieleciak, R. M.; Huber, M. L.; Kweon, C.-B.; McConnell, S. S.; Pitz, W. J.; Ratcliff, M. A., Diesel surrogate fuels for engine testing and chemical-kinetic modeling: Compositions and properties. *Energy Fuels* **2016,** 30, 1445-1461.
2. *ASTM D613 - 18a, Standard test method for cetane number of diesel fuel oil*. ASTM International: West Conshohocken, PA, 2018.
3. Hiroyasu, H.; Arai, M.; Tabata, M., Empirical equations for the sauter mean diameter of a diesel spray. *J Engines* **1989,** 98, 868-877.
4. Chehroudi, B.; Talley, D.; E., C., Visual characteristics and initial growth rates of round cryogenic jets at subcritical and supercritical pressures. *Phys of Fluids* **2002,** 14, 850.
5. Anitescu, G.; Tavlarides, L. L.; Geana, D., Phase Transitions and Thermal Behavior of Fuel-Diluent Mixtures. *Energy Fuels* **2009,** 23, 3068-3077.

6. Jianhua, T.; Satherley, J.; Schiffrin, D. J., Density and interfacial tension of nitrogen-hydrocarbon systems at elevated pressures. *Chin J Chem Eng* **1993,** 1, 223-231.

7. Zolghadr, A.; Riazi, M.; Escrochi, M.; Ayatollahi, S., Investigating the effects of temperature, pressure, and paraffin groups on the N_2 miscibility in hydrocarbon liquids using the interfacial tension measurement method. *Ind Eng Chem Res* **2013,** 52, 9851-9857.

8. Garrido, J. M.; Cifuentes, L.; Cartes, M.; Segura, H.; Mejía, A., High-pressure interfacial tensions for nitrogen + ethanol, or hexane or 2-methoxy-2methylbutane: A comparison between experimental tensiometry and Monte Carlo simulations. *J Supercrit Fluid* **2014,** 89, 78-88.

9. Reno, G. J.; Katz, D. L., Surface tension of *n*-heptane and *n*-butane containing disolved nitrogen. *Ind Eng Chem* **1943,** 35, 1091-1093.

10. Dechoz, J.; Rozé, C., Surface tension measurement of fuels and alkanes at high pressure under different atmospheres. *Appl Surf Sci* **2004,** 229, 175-182.

11. Niño Amézquita, O. G.; Enders, S.; Jaeger, P. T.; Eggers, R., Interfacial properties of mixtures containing supercritical gases. *J Supercrit Fluids* **2010,** 55, 724-734.

12. Pereira, L. M. C.; Chapoy, A.; Burgass, R.; Tohidi, B., Measurement and modelling of high pressure density and interfacial tension of (gas + *n*-alkane) binary mixtures. *J Chem Thermodyn* **2016,** 97, 55-69.

13. Chen, Z.; Xia, S.; Ma, P., Measuring surface tension of liquids at high temperature and elevated pressure. *J Chem Eng Data* **2008,** 53, 742-744.

14. Standing, M. B.; Katz, D. L., Density of Natural Gasses. *Trans Am Inst Mining Met Engrs* **1942,** 146, 140-149.

15. Rowane, A. J.; Gavaises, M.; M^{c}Hugh, M. A., Vapor-liquid equilibria and mixture densities for 2,2,4,4,6,8,8-heptamethylnonane + N2 and n-hexadecane + N2 binary mixtures up to 535 K and 135 MPa. *Fluid Phase Equilib* **2020,** 506, 112378.

16. Cahn, J. W.; Hilliard, J. E., Free energy of a nonuniform system. I. Interfacial free energy. *J Chem Phys* **1958,** 28, 258-267.

17. Liu, S. T.; Fu, D.; Lu, J. Y., Investigation of bulk and interfacial properties for nitrogen and light hydrocarbon binary mixtures by perturbed-chain statistical associating fluid theory combined with density-gradient theory. *Ind Eng Chem Res* **2009,** 48, 10734-10739.

18. Burgess, W. A.; Tapriyal, D.; Gamwo, I. K.; Wu, Y.; M^{c}Hugh, M. A.; Enick, R. M., New group-contribution parameters for the calculation of PC-SAFT parameters for use at pressures to 276 MPa and temperatures to 533 K. *Ind Eng Chem Res* **2014,** 53, 2520-2528.

19. Sauer, E.; Stavrou, M.; Gross, J., Comparison between a homo- and a heterosegmented group contribution approach based on the perturbed-chain polar statistical associating fluid theory equation of state. *Ind Eng Chem Res* **2014,** 53, 14854-14864.

20. Tihic, A.; Kontogeorgis, G. M.; von Solms, N.; Michelsen, M. L., A predictive group-contribution simplified PC-SAFT equation of state: Application to polymer systems. *Ind Eng Chem Res* **2008,** 47, 5092-5101.

21. Berry, J. D.; Neeson, M. J.; Dagastine, R. R.; Chan, D. Y. C.; Tabor, R. F., Measurement of surface and interfacial tension using pendant drop tensiometry. *J Colloid Interface Sci* **2015,** 454, 226-237.

22. Advance Software. https://www.kruss-scientific.com/products/advance-software/overview/ (March 04, 2020),

23. Gross, J.; Sadowski, G., Perturbed-Chain SAFT: An equation of state based on a perturbation theory for chain molecules. *Ind Eng Chem Res* **2001,** 40, 1244-1260.

24. Mairhofer, J.; Gross, J., Modeling of interfacial properties of multicomponent systems using density gradient theory. *Fluid Phase Equilib* **2017,** 439, 31-42.

25. Laursen, T. VLXE, V. 9.3. www.vlxe.com